Swiss Federal Laboratories for Materials Testing and Research
Überlandstrasse 129 CH-8600 Dübendorf Phone +41 (0)1 823 55 11 Fax +41 (0)1 821 62 44

EMPA

1 Machine vision

We describe a machine vision measurement head that is used to monitor the mandrel position in production of superconducting cables. Two cameras are orthogonally aligned, viewing different sections of the cylindrical part of the mandrel. The use of telecentric lenses obviates the need for recalibration after the replacement of mandrel. All parameters of rigid body motion are obtained in linear theory by using a multivariate least squares fit procedure on dynamically corresponded sets of target points that vary due to obstruction by rotating wires. A rigorous analysis of measurement uncertainty is given. [1]

2 Hardware description

2.1 Camera, lenses and illumination

B/W CCIR-cameras with standard 768 x 512 pixel resolution have been chosen. In order to minimise the size of the measurement system, compact C-mount cameras were purchased. They can be triggered and genlocked. Chipsize was chosen to be of 1/3“ equivalent. The high lateral resolution allows to use smaller and hence more compact and lightweight lenses. A field of view (FOV) of6 x 8 mm^2 was aimed at. As ambient light can strongly vary, an auto gain control (AGC) is mandatory. A shuttered operation minimises blur due to the movement of the wires in front of the mandrel.

The FOV requires a magnification of 0.6X when using a camera chip size of 3.6 x 4.8 mm^2. A working distance of 100 mm is kept in order to be in safe distance to the production site and at the same time achieving stable images. The objective is a compact and lightweight telecentric C-mount lens. Magnification is independent of object distance within the entire depth of focus. Hence, there is no need to recalibrate the lateral resolution after repositioning the system or focusing the camera.
The lens has no adjustable features, so mismanipulation or accidental mistuning are impossible. As the aperture is fixed, the camera must adjust itself to the varying illumination condition through its AGC capability. As no focus ring is provided on the lens, focussing is performed through positioning of the camera-lens system with respect to the object surface by using a translation stage.

The camera and the lens described above result in a scaling of

κ_{hor} = (0.01038± 0.00001) mm/x-pixel

κ_{vert} = (0.01042± 0.00001) mm/y-pixel

and hence a field of view (FOV) of 6.00x7.98 mm^2.

The depth of focus 2*f* is compatible with the curvature of the test object.

An illumination with 5mm white light LED and 45°-illumination cone is integrated to the camera casing. Due to space restrictions, a ring-illuminator is too large. We therefore have designed a 4-LED illumination placed in pairs on each side of the objective (Figure 1).

[1] E. Hack, D. Leroy, *Camera based monitoring of the rigid body displacement of a mandrel in superconducting cable production,* Opt. Las. Eng. **43** (2005)*3-5*, 455–474

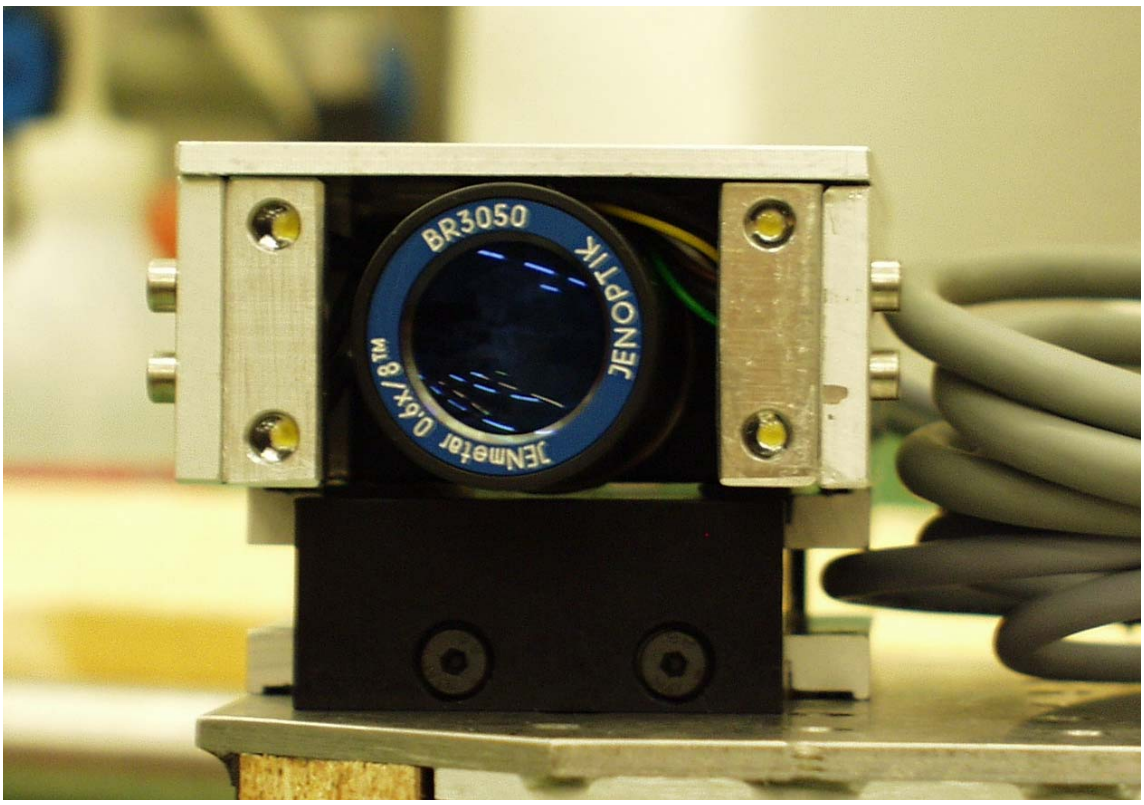

Figure 1: Front view of camera, casing and illumination block with four LEDs.

2.2 Targets

The targets (Figure 2) are used to define measurement points on the object surface. They are fabricated to customer specification and printed onto a self-adhesive white foil of thickness 0.1 mm. The target includes a scaling (1-50 mm) in order to allow for the determination of the axis-offset .

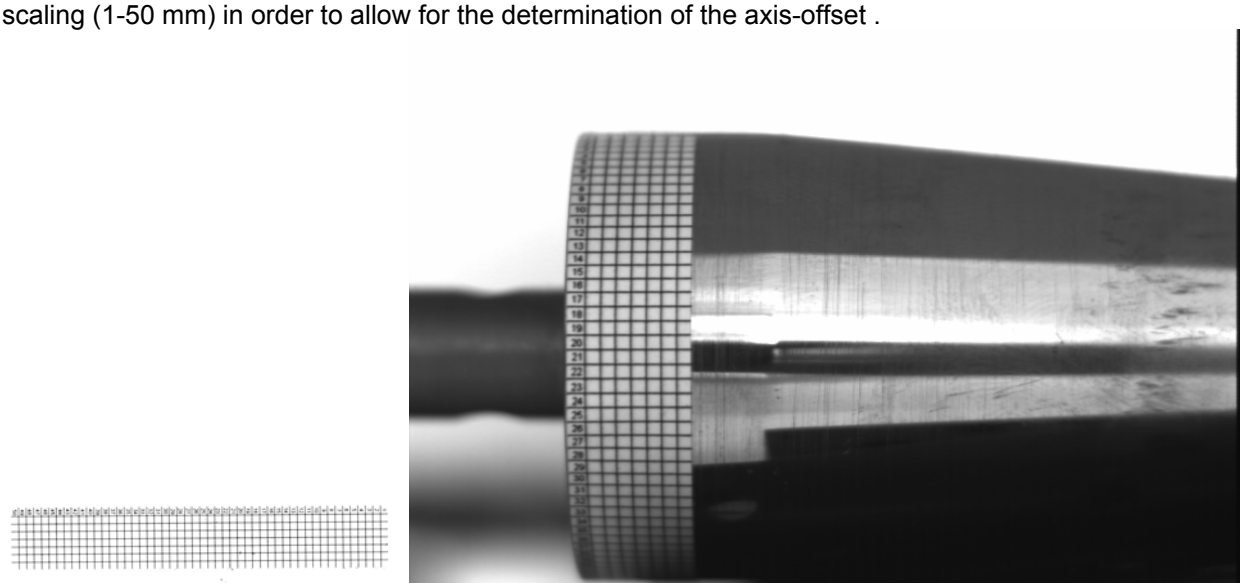

Figure 2: Target with scaling and reference grid (left). Test object with target (right).

2.3 Mechanical mounting

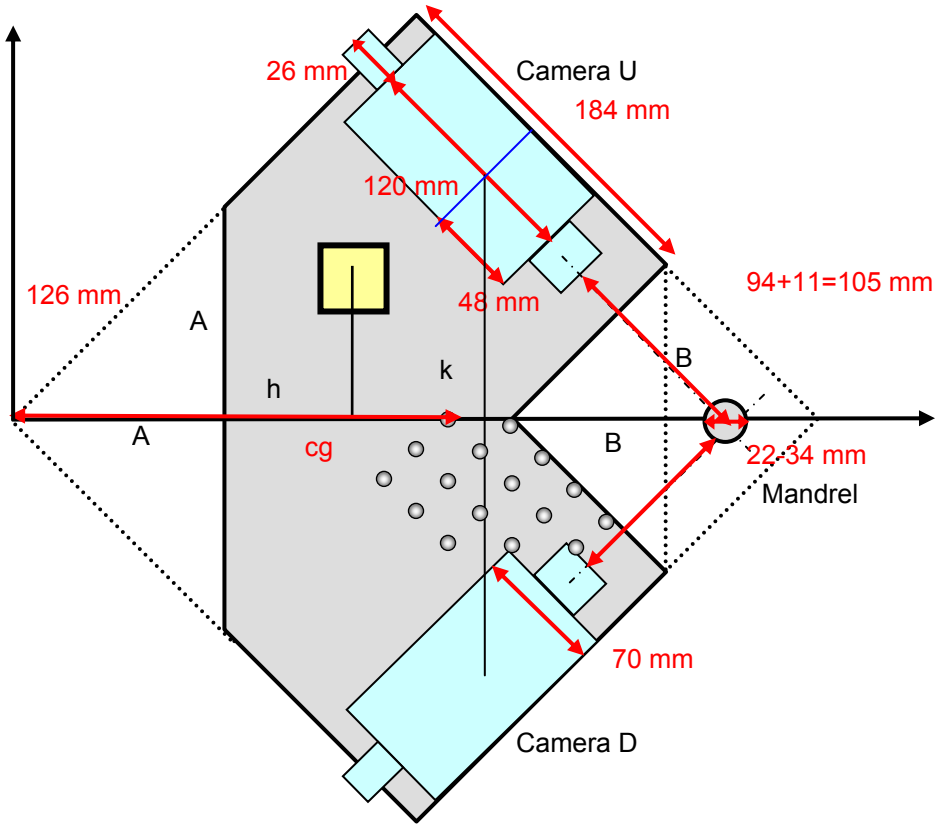

Figure 3: Mechanical mounting of the two camera units to the breadboard, schematic.

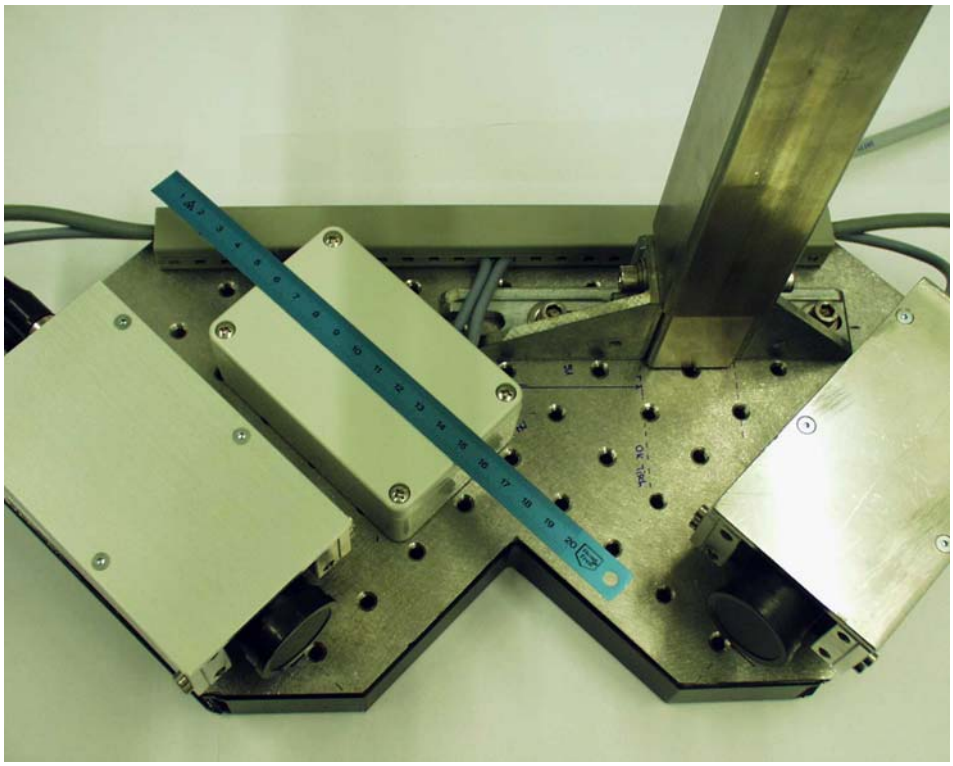

Figure 4: Measurement head with breadboard, two cameras in their casing, electrical connector box, and mounting tube attached with angle brackets.

3 Description of the evaluation algorithm

3.1 General

The displacement of the mandrel can be parameterised as a rigid body displacement of a cylinder with six degrees of freedom (section 5.2). The target displays a grid of 1mm squares the crossing points of which serve as measurement points. The image analysis localises the camera co-ordinates of these points by image correlation. Using a telecentric lens these camera co-ordinates are the parallel projection of the target points along the line of sight (i.e. the optical axis of the camera) onto the CCD sensor plane.
Once the co-ordinates of the measurement points are known, they are compared to the reference position of the test object in order to calculate the displacement values. Note that the sets of visible target points may vary from image to image due to the wires crossing the field of view during production.
Due to mounting inaccuracies, we cannot assume that the optical axes of the cameras intersect the mandrel cylinder axis. Hence, we must assume an axis-offset and determine its value before evaluation.
In order to take into account the two sets of points from both cameras, a unified evaluation procedure based on a multivariate least-squares analysis is applied. The basic equations relating the displacement values to the rigid-body parameters are derived. The mathematics of the least squares fit of the rigid body parameters, taking into account the unified set of measured points is explained. Finally, a measurement uncertainty analysis is performed.

3.2 Rigid body displacement

The separation of a rigid body displacement into translation and rotation is not unique. Hence, we may define an arbitrary point as the centre of rotation. If we choose the origin of the co-ordinate system to be this reference point, the rigid body displacement can be written as

$$\mathbf{v}(\mathbf{x}) = \mathbf{x}' - \mathbf{x} = \begin{pmatrix} t_x - \alpha_z y - \alpha_y z \\ t_y + \alpha_z x - \alpha_x z \\ t_z + \alpha_y x + \alpha_x y \end{pmatrix} \tag{1}$$

We define the intersection of the plane spanned by the two camera optical axes and the cylinder axis as the origin of the co-ordinate system.
A point **P** on the surface of the cylindric test object can be parameterised by (r, φ_P, z_P). The z-co-ordinate remains unchanged in any parallel projection (as with telecentric lenses) onto a plane parallel to the z-axis. By definition, the cameras point onto the y-axis at an angle of φ_U (ca. 45° from x-axis) and φ_D (ca. 135° from x-axis). They may, however, be off-centre from the z-axis by an amount s_U and s_D, respectively, called axis-offset. This off-axis observation is vital to achieve a good separation of the various components of rigid body displacements.
U and D designate indices for the upper camera (UP) and lower camera (DOWN), respectively.The surface point co-ordinates can be reconstructed from the camera co-ordinates by

$$\begin{aligned} y &= \sqrt{r^2 - (\eta_U + s_U)^2}\,\sin\varphi_U + (\eta_U + s_U)\cos\varphi_U \\ x &= \sqrt{r^2 - (\eta_U + s_U)^2}\,\cos\varphi_U - (\eta_U + s_U)\sin\varphi_U \end{aligned} \tag{2}$$

The same formulae apply for the lower camera D, when respecting the sign of γ. While the camera co-ordinates are readily read from the pixel position, the offset s from the cylinder axis has to be determined from the actual field of view.

To express the displacement of a target point in the camera image we have in terms of the parameters of rigid body displacement

$$\begin{aligned} \Delta\xi_U &= t_z + \alpha_y x + \alpha_x y \\ \Delta\eta_U &= (t_y + \alpha_z x - \alpha_x z)\cos\varphi_U - (t_x - \alpha_z y - \alpha_y z)\sin\varphi_U \end{aligned} \tag{3}$$

Every measurement point provides two equations for the determination of the six parameters of rigid body displacement.

3.3 Least-squares evaluation of the parameters of rigid body displacement

The sum of residual squares is to be minimised by choosing the appropriate values for the parameters. The sums extend through the entire set of measurement points N_U and N_D of the upper and lower camera, respectively. We use unweighted sums, i.e. we assume all measurement points to have the same uncertainty. To find the minimum of the sum, all partial derivatives with respect to the six parameters (A_0, A_1, ..., A_5) of rigid body displacement

$$\mathbf{A} = \begin{pmatrix} t_z & t_+ & t_- & \delta_z & \delta_+ & \delta_- \end{pmatrix}^{tr} \tag{4}$$

are set equal to zero. The least squares procedure finally leads to the matrix equation

$$\underline{\mathbf{N}}\mathbf{A} = \mathbf{Y} \tag{5}$$

with

$$\mathbf{Y} = \begin{pmatrix} [\Delta\xi_U] + [\Delta\xi_D] \\ -[\Delta\eta_D] \\ -[\Delta\eta_U] \\ \left[\Delta\eta_U\sqrt{1-\tau_U{}^2}\right] + \left[\Delta\eta_D\sqrt{1-\tau_D{}^2}\right] \\ \left[\Delta\xi_U\sqrt{1-\tau_U{}^2}\right] - [\Delta\xi_D\tau_D] + [\Delta\eta_D\varsigma_D] \\ [\Delta\xi_U\tau_U] - [\Delta\eta_U\varsigma_U] + \left[\Delta\xi_D\sqrt{1-\tau_D{}^2}\right] \end{pmatrix} \tag{6}$$

The square brackets are short for the respective summations through the number of measurement points for cameras U and D. The normal matrix is symmetric and given by

$$\underline{\mathbf{N}} = \begin{pmatrix} (N_U + N_D) & 0 & 0 & 0 & \left(\left[\sqrt{1-\tau_U{}^2}\right] - [\tau_D]\right) & \left([\tau_U] + \left[\sqrt{1-\tau_D{}^2}\right]\right) \\ 0 & N_D & 0 & -\left[\sqrt{1-\tau_D{}^2}\right] & -[\varsigma_D] & 0 \\ 0 & 0 & N_U & -\left[\sqrt{1-\tau_U{}^2}\right] & 0 & [\varsigma_U] \\ 0 & -\left[\sqrt{1-\tau_D{}^2}\right] & -\left[\sqrt{1-\tau_U{}^2}\right] & \left([1-\tau_U{}^2] + [1-\tau_D{}^2]\right) & \left[\varsigma_D\sqrt{1-\tau_D{}^2}\right] & -\left[\varsigma_U\sqrt{1-\tau_U{}^2}\right] \\ \left(\left[\sqrt{1-\tau_U{}^2}\right] - [\tau_D]\right) & -[\varsigma_D] & 0 & \left[\varsigma_D\sqrt{1-\tau_D{}^2}\right] & \left([1-\tau_U{}^2] + [\tau_D{}^2] + [\varsigma_D{}^2]\right) & \left(\left[\tau_U\sqrt{1-\tau_U{}^2}\right] - \left[\tau_D\sqrt{1-\tau_D{}^2}\right]\right) \\ \left([\tau_U] + \left[\sqrt{1-\tau_D{}^2}\right]\right) & 0 & [\varsigma_U] & -\left[\varsigma_U\sqrt{1-\tau_U{}^2}\right] & \left(\left[\tau_U\sqrt{1-\tau_U{}^2}\right] - \left[\tau_D\sqrt{1-\tau_D{}^2}\right]\right) & \left([1-\tau_D{}^2] + [\tau_U{}^2] + [\varsigma_U{}^2]\right) \end{pmatrix} \tag{7}$$

Eq. (5.35) is solved for $\mathbf{A}$ by using the inverse of this normal matrix $\mathbf{N}$.

Figure 5 shows the result of a calibration measurement performed for pure translations of ± 0.1 mm along x, y, and z-direction. Note that the noise in tx is remarkably higher than in tz or ty, and correlated with αz. This fact is substantiated by the uncertainty values given by the elements of the covariance matrix below.

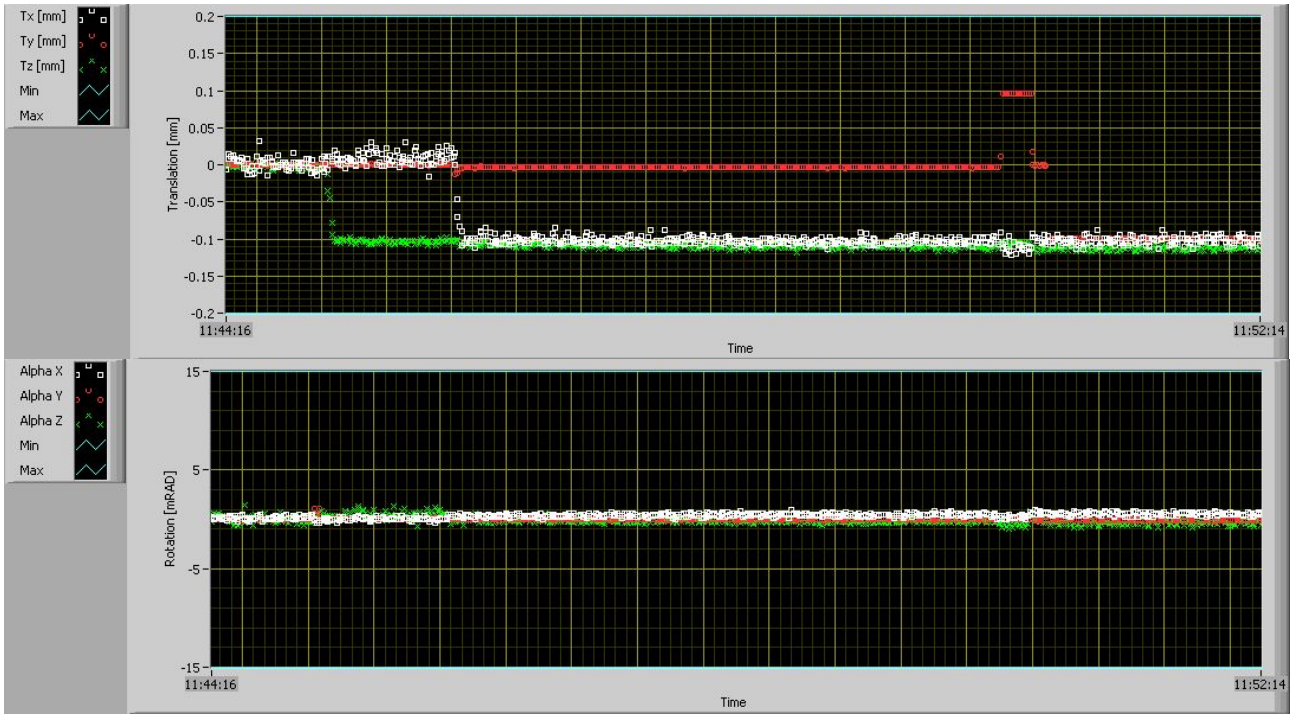

Figure 5: Calibration of the translation measurements (top). Note that the rotation values are not substantially affected (bottom)

3.4 Measurement uncertainty

All measurement values have uncertainties associated to the identification of the target points. However, the dimensionless camera co-ordinates have themselves measurement uncertainties. As is known, we may calculate from them an **equivalent uncertainty** of the displacements of the camera co-ordinates, which has to be added to the identification uncertainty according to the error propagation rules. Further, we must take into account the non-ideal real situation. This is dominated by geometrical uncertainties.

$$u^2(\Delta\xi) = u^2(\Delta\xi, ident) + u^2(\Delta\xi, equivalent) + u^2(\Delta\xi, geometry) \quad (8)$$

and similar for the displacement $\Delta\eta$.

The estimation of the measurement uncertainty for the translation and rotation values is therefore made step by step, according to the ISO “Guide to the Expression of Uncertainty in Measurement”.

- Measurement uncertainty of the displacement measurement value determination due to the correlation algorithm.
- Equivalent uncertainty due to
  - Uncertainty of the relative camera co-ordinates, comprising uncertainty of
    - Camera co-ordinates
    - Axis offset s
    - Radius r
- Geometrical uncertainty
  - Uncertainty of camera angle φ
  - Non-coplanarity of the two cameras
  - Temperature effects

Covariance matrix

The measurement uncertainties (variances and covariances) are given by the inverse of the normal matrix, multiplied by the variance of the uncertainty of a single measurement value. We assume that all measurement uncertainties are equal A typical normal matrix obtained during the calibration of the system is:

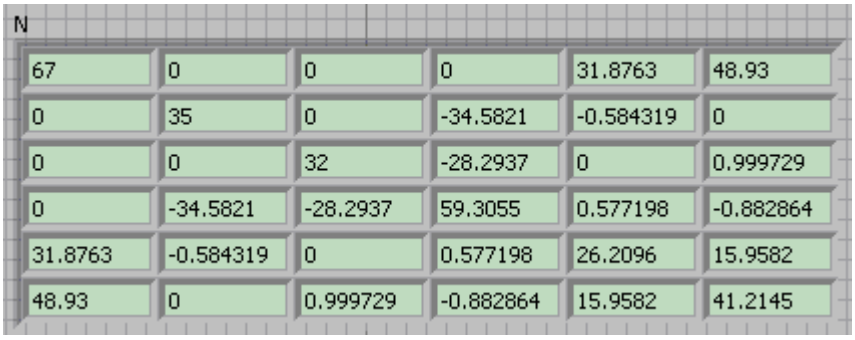

Figure 10: Values of the normal matrix coefficients obtained during calibration.

In this case, there are 35 and 32 target points identified in the images of the lower and upper camera, respectively. The corresponding covariance matrix in the back transformed parameters, is

Parameter	Back transformed Covariance Matrix					
tz	**1.882**	**0.044**	**-0.052**	**0.014**	**-2.107**	**0.390**
tx	**0.044**	**14.680**	**0.810**	**11.066**	**-0.049**	**0.011**
ty	**-0.052**	**0.810**	**0.076**	**0.614**	**0.059**	**-0.011**
δz	**0.014**	**11.066**	**0.614**	**8.359**	**-0.016**	**0.003**
δx	**-2.107**	**-0.049**	**0.059**	**-0.016**	**2.381**	**-0.427**
δy	**0.390**	**0.011**	**-0.011**	**0.003**	**-0.427**	**0.141**

The variance of the parameter tx (i.e. the diagonal element of the covariance matrix) is higher by a factor of up to fifteen than that of the single measurement value. Further, there is strong correlation between tx and δz as well as some correlation between tz and δx.
Since it is not reasonable to make an uncertainty analysis for each measurement, we assume that the idealised covariance matrix is valid for all measurements and that it roughly scales with the number of detected points.

Compilation of measurement uncertainties for the two components of camera coordinate displacements

Influence parameter	**Formula**	**Assumptions and values**	**Contribution to $u^2(\Delta\xi)$ r=11 mm**	**Contribution to $u^2(\Delta\xi)$ r=17 mm**
Identification of target point	$u^2(\Delta\xi, ident) = (0.003mm)^2$		9 x 10^{-6} mm^2	9 x 10^{-6} mm^2
Dimensionless camera co-ordinate	$u^2(\tau) \approx \frac{u^2(s)}{r^2}$	$u^2(s) < (0.26mm)^2$ r = 11 mm $u^2(s) < (0.63\ mm)^2$ r = 17 mm		
Equivalent uncertainty	$u^2(\Delta\xi, equivalent) = \langle\alpha_r^2\rangle\left(1+\frac{s^2}{r^2}\right)u^2(s)$	$\langle\alpha_i^2\rangle = (8\ mrad)^2$ $\frac{s^2}{r^2} = \frac{1}{9}$	5 x 10^{-6} mm^2	28 x 10^{-6} mm^2
Camera angle	$u^2(\Delta\xi,\varphi) = r^2\langle\alpha_r^2\rangle u^2(\varphi)$	$u^2(\varphi) = (17mrad)^2$	2 x 10^{-6} mm^2	5 x 10^{-6} mm^2
Temperature change	$u^2(\Delta\xi, temperature) = (0.006mm)^2$	u(T)=5°C	36 x 10^{-6} mm^2	36 x 10^{-6} mm^2
Total	$u^2(\Delta\xi)$		52 x 10^{-6} mm^2	78 x 10^{-6} mm^2

Influence parameter	**Formula**	**Assumptions and values**	**Contribution to $u^2(\Delta\eta)$ r=11 mm**	**Contribution to $u^2(\Delta\eta)$ r=17 mm**
Identification of target point	$u^2(\Delta\eta, ident) = (0.003mm)^2$		9 x 10^{-6} mm^2	9 x 10^{-6} mm^2
Dimensionless camera co-ordinate	$u^2(\varsigma) = \frac{1}{r^2}(0.010\ mm)^2$			
Equivalent uncertainty	$u^2(\Delta\eta, equivalent) = \langle\alpha_r^2\rangle r^2\ u^2(\varsigma) + \langle\alpha_z^2\rangle\frac{s^2}{r^2}u^2(s)$	$\langle\alpha_i^2\rangle = (8\ mrad)^2$ $\frac{s^2}{r^2} = \frac{1}{9}$	1 x 10^{-6} mm^2	3 x 10^{-6} mm^2
Camera angle	$u^2(\Delta\eta,\varphi) = \left[\langle t_r^2\rangle + 0.025\, r^2\langle\alpha_r^2\rangle\right]u^2(\varphi)$	$\langle t_r^2\rangle = (0.13\ mm)^2$	5 x 10^{-6} mm^2	8 x 10^{-6} mm^2
Non-coplanarity	$u^2(\Delta\eta, z) = \langle\alpha_r^2\rangle u^2(z)$	$u^2(z) = (0.5mm)^2$	16 x 10^{-6} mm^2	16 x 10^{-6} mm^2
Temperature change	$u^2(\Delta\eta, temperature) = (0.002\ mm)^2$	u(T) = 5°C	4 x 10^{-6} mm^2	4 x 10^{-6} mm^2
Total	$u^2(\Delta\eta)$		35 x 10^{-6} mm^2	40 x 10^{-6} mm^2

We may therefore assume the combined uncertainty of the camera displacement values to be $u(\Delta\xi) = 0.008\,mm$ and $u(\Delta\eta) = 0.006\,mm$

Weighting both uncertainties equal, the variance of the measurement of the camera displacement is estimated to be 50 x 10^{-6} mm^2 corresponding to a measurement uncertainty of 0.007 mm (1σ).

Taking the covariance matrix given in section 5.7.2 and multiplying with this variance gives

Parameter	Back transformed Covariance Matrix (idealised case) [µm²]					
tz	92	0.0	0.0	0.0	-102	0.0
tx	0.0	670	0.0	506	0.0	0.0
ty	0.0	0.0	1.4	0.0	0.0	0.0
δz	0.0	506	0.0	384	0.0	0.0
δx	-102	0.0	0.0	0.0	113	0.0
δy	0.0	0.0	0.0	0.0	0.0	3.7

Usually the diagonal matrix elements are taken as an estimate of the measurement uncertainty of the parameters.

Table 8: Combined and expanded uncertainty of the parameters of rigid body displacement.

Measurement uncertainty [µm]				Expanded Uncertainty (k=2, covering a range of 95% when a normal distribution is assumed)		
		r = 11 mm	r = 17 mm			
u(tz) = 9.6				**U(tz) =**	**19**	**µm**
u(tx) = 26				**U(tx) =**	**52**	**µm**
u(ty) = 1.2		**[mrad]**	**[mrad]**	**U(ty) =**	**3**	**µm**
u(δz) = 20	**u(αz) =**	**1.78**	**1.15**	**U(αz) =**	**4**	**mrad**
u(δx) = 11	**u(αx) =**	**0.97**	**0.63**	**U(αx) =**	**2**	**mrad**
u(δy) = 1.9	**u(αy) =**	**0.17**	**0.11**	**U(αy) =**	**1**	**mrad**